The University Of Sheffield.

Modelling the impact of deep brain stimulation on the basal ganglia output to the thalamus

Degree: MSc Cognitive & Computational Neuroscience

Department: Department of Psychology, The University of Sheffield, Sheffield, United Kingdom

Registration number: 190218331

Supervisor(s): Dr. Robert Schmidt & Dr. Mohammadreza Mohagheghi Nejad

Date of submission: 08/2020

Abstract

Contents

1 Introduction

1.1 Parkinson's disease and deep brain stimulation

Parkinson's disease (PD) is a age-related progressive neurodegenerative disorder known for its share of the elderly population affected by it[1]. The disease is characterised for its most notorious pathology: the selective degenerative death of dopaminergic neurons in the substantia nigra pars compacta (SNpc)[2].

It is thought that the depletion of dopamine in the basal ganglia (BG) could be the cause behind excessive neuronal activity synchronisation seen in PD patients[3]. While the exact cause behind motor dysfunction in PD, such as muscle rigidity, tremors and difficulty in initiating and ending volitional movements is not yet well known, it is theorised that this pathological synchronisation not seen in healthy individuals could be the cause behind it[4].

Deep brain Stimulation (DBS) is a surgical procedure that is used to treat the motor dysfunctions in PD. Electrodes are implanted in the BG in order to deliver high-frequency stimulation via electrical pulses, where the subthalamic nucleus (STN) is usually the main target[5]. This procedure has been proved to vastly improve the motor symptoms in PD[6].

Despite the widespread use of this procedure, the exact effects that the high-frequency stimulation produces in order to subside the motor dysfunctions in PD is not well known and the observable results vary from individual to individual. Results have shown both increases[7] and decreases[8] in the substantia nigra pars reticulata (SNr) firing rates, and other studies have shown heterogeneous responses, such as subsets of neurons who can increase their firing rates and burst rates, subsets that have their firing rate and burst rate decreased, and subsets which are not affected by the DBS[9]. Simulations of DBS on the basal ganglia output also showed a mixture of responses on it, showing a "network effect" caused by the DBS, which may be the driving cause behind the effectiveness of DBS[10].

Hahn et al's results are of special interest, since they showed that despite both rhesus monkeys in the study displayed improvement with DBS, only one of them had relevant changes in firing and burst rate. Hahn argues that this implies that while firing and bursting rate as an affect of DBS may be involved in

the improvement of motor symptoms, they are not the only factors that cause such progress. Hahn would then attribute such improvement to physiological changes that are not currently known.

However, Hahn, amongst others previously cited, does not take into account the correlation of the basal ganglia output and how it is affected by DBS as a possible factor in his study, omitting what could be an important factor that could explain the success behind DBS.

1.2 The basal ganglia output, correlation and transmission quality

The basal ganglia output is a structure formed by subcortical nuclei which is thought to control and execute voluntary movements[11]. Motor signals are transmitted via the basal ganglia output, where the activity of the globus pallidus internus (GPi) and the SNr is decreased, disinhibiting the motor thalamus (Mthal)[13].

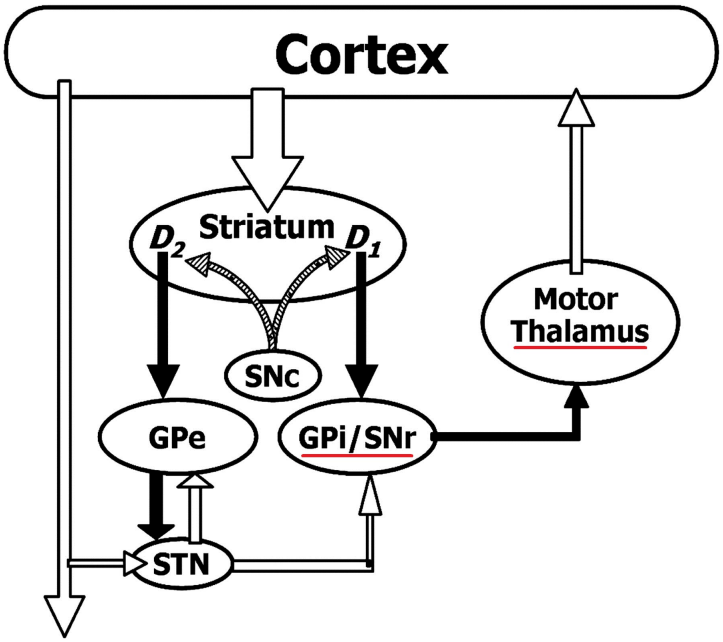

Figure 1. *Primate basal ganglia model.* Image taken from Rubchinsky et al [12]. In this model the basal ganglia output and the motor thalamus have been underlined to show the connections in the BG. Note how the STN and the Striatum are connected to the basal ganglia output. In this figure black arrows denote inhibition and white arrows excitation.

When motor signals are propagated in order to execute voluntary movements, the striatum inhibits the

activity of the basal ganglia output. Due to the fact that the motor thalamus is always under constant inhibition from the basal ganglia output, when the BG output decreases its usual high-frequency firing rate, the motor thalamus is able to transmit the corresponding motor signal[14].

Although there are several possible methods via which the variation of BG firing rate can induce motor signal transmission through the Mthal this project will focus on rebound spikes. Sudden stops in the BG output are capable of eliciting rebound spikes in the Mthal due to releases after long periods of hyperpolarisation without any additional excitation[15]. The Mthal neurons are capable of such rebound spiking by virtue of their T-type Ca^{2+} channels[16].

Research has shown that correlation in the basal ganglia output can severely influence the transmission of motor signals in the Mthal due to this rebound spiking mechanism[17]. The concept of correlation in the basal ganglia output refers to the probability of two or more spiketrains having spikes at the same time. A correlation of 0% would mean that such spiketrains never have spikes that fire simultaneously, but a correlation of 0.5 (or 50%) would mean that the spikes from such spiketrains have a 50% chance of firing at the same time. Mohammadreza et al found that such correlation creates unwanted stops in the BG output, causing rebound spikes to happen even without the presence of excitation (see figure 2).

Mohammadreza introduced the concept of transmission quality (TQ) to measure the clearness of motor signal transmission. An ideal scenario would be for the Mthal to produce a rebound spike once: when the BG output reduces its activity due to the movement-related activity and naturally produces a pause. Any other rebound spike in the Mthal produces a noisy transmission, which in turn hinders the decoding of thalamic activity, resulting in a decrease of accuracy of motor transmission. The TQ is calculated by observing how many rebound spikes occur out of the intended. For example, a ”perfect” TQ would be 1, which indicates that the only rebound spikes that happened where associated with volitional movements, and a TQ of 0.5 indicates that half of these spikes were not intentional.

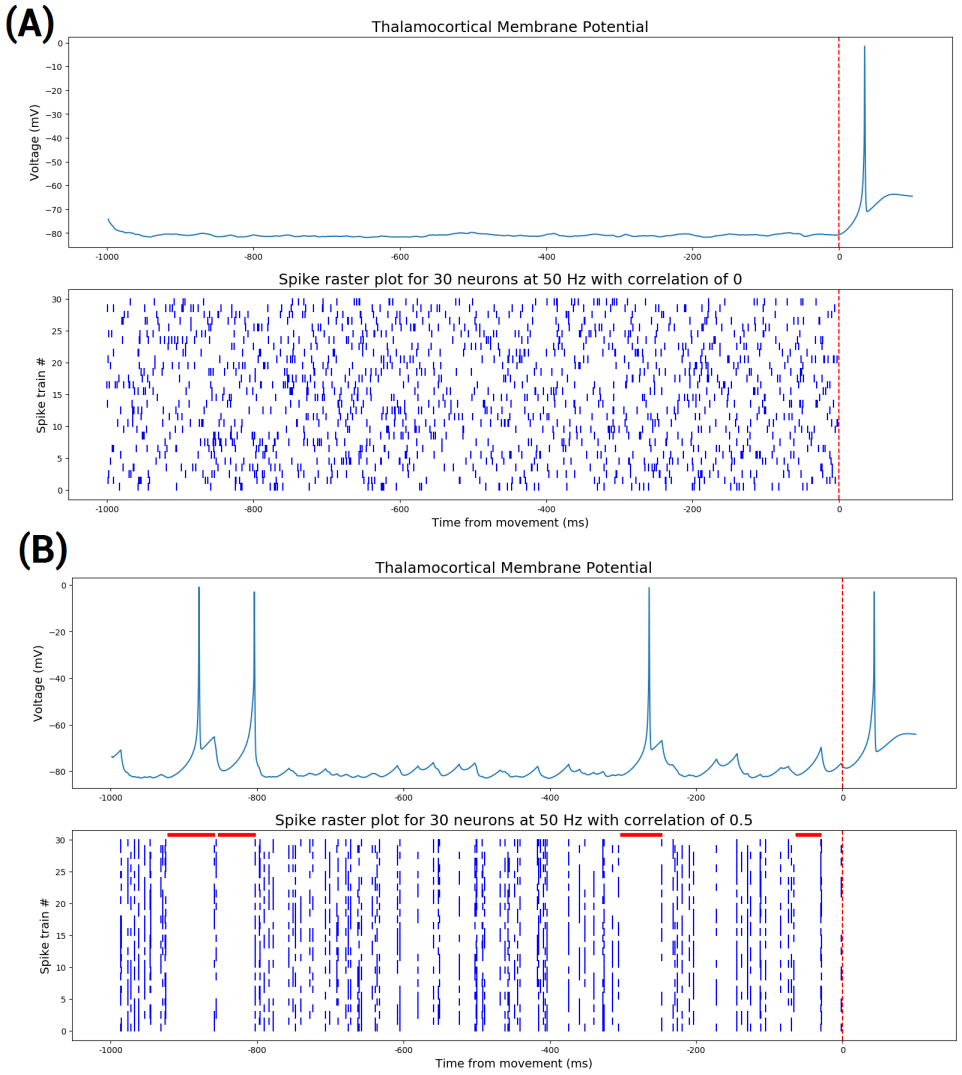

Figure 2. *The impact of correlation in the BG output*. In both A and B the raster plot in the bottom is a simulated set of 30 spiketrains from the SNr, and the upper part is a simulated thalamocortical neuron with the 30 spiketrains as its only input. In both scenarios, a movement-related decrease in SNr activity is introduced at the 1 second mark (denoted by a red dashed line). (A) The SNr with a correlation of 0 elicits one single rebound spike at the desired moment, with a TQ of 1, since no other spike can be observed. (B) In this case, the SNr has a correlation of 0.5, which creates pauses that are capable of eliciting undesired rebound spikes. The red rectangles seen in the top of the rasterplot indicate pauses have a duration of 35 ms or more, which are capable of generating rebound spikes. In this case, the TQ would be 0.25, since out of 1 intended spike, 4 have occurred.

1.3 Plan of investigation

Knowing from Mohammadreza's work that correlation affects TQ, and that PD patients have been observed with pathological correlation in the BG output, comes our research question: What is the impact of deep brain stimulation on the correlation of the basal ganglia output? Since the efficacy and the exact functioning of DBS is not well known, the evolution of correlation before and during DBS may give an insight into the working of DBS and possibly suggest why some studies show different results for the same types of DBS.

A list of the main objectives would be:

- Observing how correlation in the BG output changes during DBS
- Studying the interplay of firing rate and correlation during DBS
- Studying different scenarios in DBS, such as groups of neurons who become de-correlated, or groups of neurons who are not affected by DBS
- Analysing the impact of correlation on transmission quality

In order to achieve such objectives, a series of simulations will be run, simulating a thalamocortical neuron with thirty different input spike trains from the SNr. In these simulations, DBS will be imitated by altering the firing rates of the SNr spiketrains and the data of the resulting thalamocortical membrane will be collected and later visualised and analysed. Such data will be compared to a "healthy" scenario where there is no correlation in the SNr and compared with biological data from studies such as Hahn et al's (2008).

A first hypothesis suggests that an increase of firing rate int the SNr caused by DBS would theoretically increase the TQ since more spikes mean that there will be less pauses between suck spikes and therefore less chances for unintentional rebound spikes to happen. Mohammadreza's work also shows that uncorrelated activity improves the TQ, so it was also hypothesised that if correlation decreases in such simulations, the TQ will improve. However, the interplay between firing rate and correlation could have many different effects, so there was no clear hypothesis in regard to such interplay, but different

possibilities were taken into account such as the existence of a limit in which the increase of firing rate is effective where the correlation is simply too high for DBS to take effect, or that both firing rate and correlation need to change at the same time in order to see a substantial benefit in TQ.

2 Methods

2.1 Thalamocortical neuron model and input spike trains

For our DBS simulations we will recreate a thalamocortical neuron with thirty SNr inputs, as in Mohamaddreza's work. The thalamocortical neuron will consist of a Hodgkin-Huxley model with three different ionic currents apart from its leak current (I_L): Na^+, K^+ and T-type Ca^{+2} currents (I_{Na}, I_k and I_T respectively). The only input to such thalamocortical neuron will be inhibitory spiketrains from the SNr, which are generated via a poisson process.

In order to simulate correlation in such spiketrains with a firing rate f and a correlation of ϵ a multiple-interaction process[18] was used: A single Poisson spike train with a rate of $r = f/\epsilon$ is generated and referred to as the mother spike train. For our process we need a mother spike train with exactly f/ϵ spikes. In order to accomplish this, the mother spike generation process is repeated until a mother spike train with the desired amount of spikes is generated. Once we have the desired mother spike train, we select r_{corr} random spikes from the mother spike N times, in order to generate N poissonian spike trains with a rate of r_{corr} and with a correlation of ϵ.

2.2 DBS simulation parameters

In order to simulate DBS a baseline scenario was set, where 30 SNr spiketrains with a firing rate of 50 Hz had varying correlations from 0.3 to 1, in order to represent different degrees of severity of Parkinson's disease. Correlations from 0 to 0.2 were not included, since the transmission quality with such parameters was always 1, indicating that there was no deterioration of motor signal transmission (see figure 3).

All the simulations where different scenarios where the DBS affected differently our baseline scenario by increasing the firing rate of the SNr spiketrains. This was done by changing the values of two different parameters:

- Number of neurons affected: To represent the heterogeneous effect of DBS and how it can affect different numbers of neurons, the number of SNr spike trains affected by the DBS frequency

increase varied from 1 to 30 neurons in steps of 1 neuron for a total of 30 experiments. These affected neurons are the ones that have their firing rate increased from their baseline firing rate of 50 Hz, while the other unaffected neurons remain at the baseline firing rate.

- Firing rate: To represent the varying effect of the DBS, the increase in firing rate provoked by the DBS went from an increase of 1 to 40 Hz in steps of 1 Hz, meaning that the frequency was increased from 51 to 90 Hz for 40 different scenarios. In each one of these scenarios, the number of neurons that would have their frequency increased would vary as well, as explained in the previous parameter. The baseline firing rate and the increases from DBS where obtained from Hahn's study in monkeys[9]

To illustrate, a simulation where the firing rate is increased to 70 Hz and the number of neurons affected by the DBS is 20 would consist of: 10 neurons who remain at the baseline firing rate of 50 Hz and 20 neurons who have their firing rate increased to 70 Hz.

For all simulations the $G_{SNr \to TC}$ inhibitory strength was always fixed at 0.7 since transmission quality does not depend inhibitory strength as long as the inhibition could warrant rebound spikes on their own [17]. The timestep of the simulation was set at 0.01 ms, the simulation lasted 1.5 seconds and the time when the SNr spike train activity stopped to simulate a volitional motor signal was at the 1 second mark. All simulations which had a unique combination of firing rate and number of neurons had varying degrees of correlation from 0.3 to 1 for all spike trains. Since the simulations are stochastic, each simulation had a total of 10 trials to avoid obtaining unreliable results.

These simulations would output the transmission quality, the total number of rebound spikes, the spike times for all spike trains and the voltage values of the thalamocortical membrane. Rebound spikes were identified by calculating the number of peaks that had a minimum peak height of -40 mV.

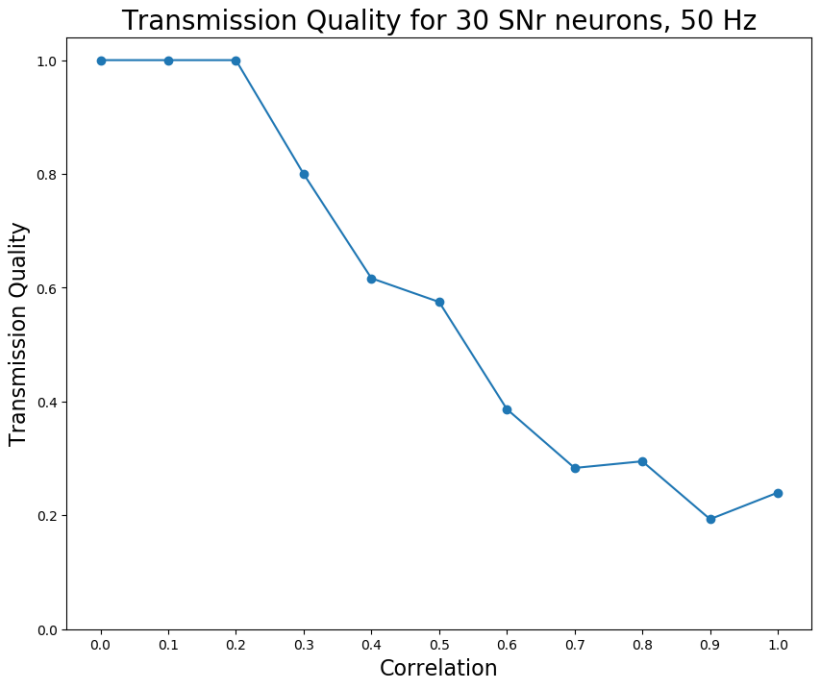

Figure 3. *Transmission quality of the baseline scenario*. This graph shows the evolution of the Transmission Quality for the different values of correlation in our baseline scenario. As it can be seen, for values of correlation up to 0.2 the transmission quality does not drop from 1, meaning that we are not interested in such cases, since there would be no necessity to apply DBS and improve such transmission quality. We could qualify such correlation values as "healthy" meaning that we are only interested in correlation values from 0.3 to 1. This transmission quality data was generated for all the simulations that have been described previously.

2.3 Correlation and decorrelation

In order to have all 30 neurons from the simulations be correlated despite that one group of neurons would always remain at baseline firing rate and the other would have their firing rate increased a method similar to the multiple-interaction process was used: All 30 spike trains were generated with their firing rate as the highest between the two groups, and for the group of neurons that remained at baseline frequency, 50 spikes were kept from such spiketrains, deleting the others. If we use the same example as before, where 10 neurons remain at 50 Hz and 20 neurons have their firing rate increased to 70 Hz, the process would be:

1. Create 30 spike trains with a firing rate of 70 Hz with the process described in section 2.1

2. For the first 10 spike trains, delete 20 random spikes from each spike train so that all 10 remaining spike trains have a baseline firing rate of 50 Hz

3. Leave the other 20 spike trains at 70 Hz

However, this simulated correlation would not suffice for scenarios where the DBS might decorrelate one group of spiketrains from the other. In order to simulate active decorrelation, that is, both groups of spiketrains are correlated amongst themselves but not with the other, a different stochastic process must be generated for each group of spiketrains. This is achieved by having each group create a mother spike train and draw spikes from it, as described in section 2.1.

2.4 Data analysis and Software packages

The simulations with the thalamocortical model neuron and the Poisson input spike trains were run in MATLAB R2016b. where Simulink was used to simulate the model neuron. All the scripts that controlled the creation of spike trains and that handled all different simulations were written in MATLAB. Since the simulations were very time consuming, they were run in the University of Sheffield's Iceberg central high-performance computing cluster.

The analysis and visualisation of the data obtained in the simulations was written on Python 3.7 scripts, which heavily relied on Scipy (in order to transform MATLAB data to analyse it in Python), Numpy (Python numerical computing package tool with built in matrix operations) and Matplotlib (Python multipurpose visualisation and plotting package).

3 Results

3.1 Decorrelation plays a role in transmission quality

In order to simulate scenarios where DBS affects a group of neurons by decorrelating it from the rest of the neurons and by increasing its firing rate, the process described in section 2.3 was followed. The group of decorrelated neurons will be the one with the corresponding frequency increase, while the other group remains at baseline frequency of 50 Hz.

As it was expected, by having two groups of neurons originate from different stochastic processes (both groups of neurons drew their spikes from different mother spikes), while the neurons in the groups where correlated among themselves at the desired correlation level, the correlation between neurons from different groups where practically 0 (see figure 4).

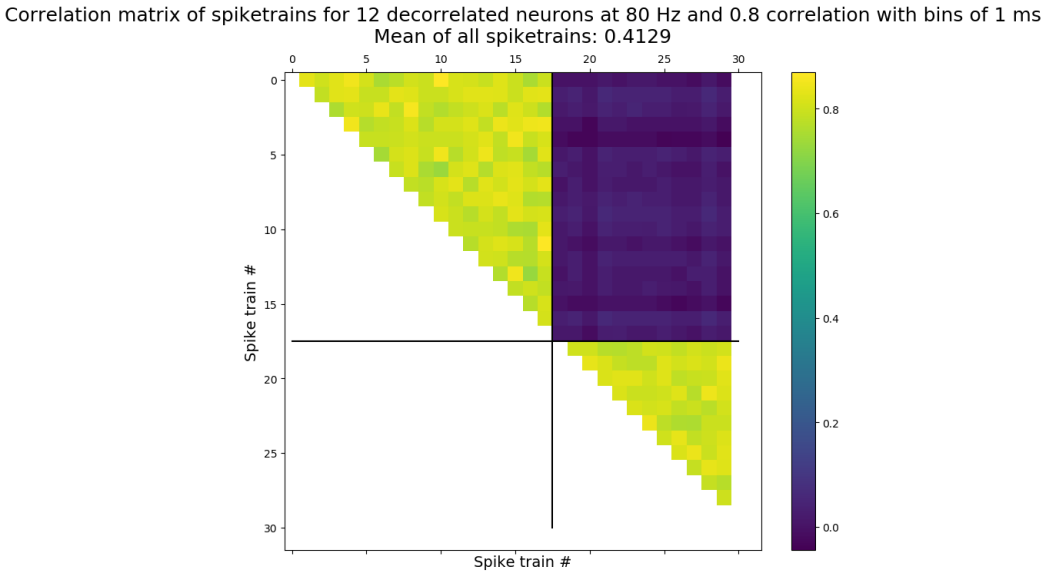

Figure 4. *Correlation matrix for 12 decorrelated neurons at 80 Hz.* Correlation values range from 0 to 1. The black lines separate the two groups of neurons: the quadrant in the upper left generated by the black lines corresponds to the 18 neurons who have remained at baseline frequency of 50 hz, and the bottom right quadrant corresponds to the neurons who have had their firing rate increased to 80 Hz. The top right quadrant are the correlations between the neurons from the different groups. Bins of 1 ms were used for the correlation matrix an the correlation for this experiment was 0.8. The ”mean of all spiketrains” indicates the average between all spiketrain correlations (mean of all the values shown in the figure)

In the example presented in figure 4 it can be seen how the overall mean of all the spiketrains has been reduced from 0.8, which was the specified correlation set as a simulation parameter, to 0.4219. Since the processes in the simulations are stochastic, we can see small variations in the correlation matrix between the groups, but the correlations of both groups are 0.802 for the baseline group and 0.803, while the correlation between both groups is 0.01.

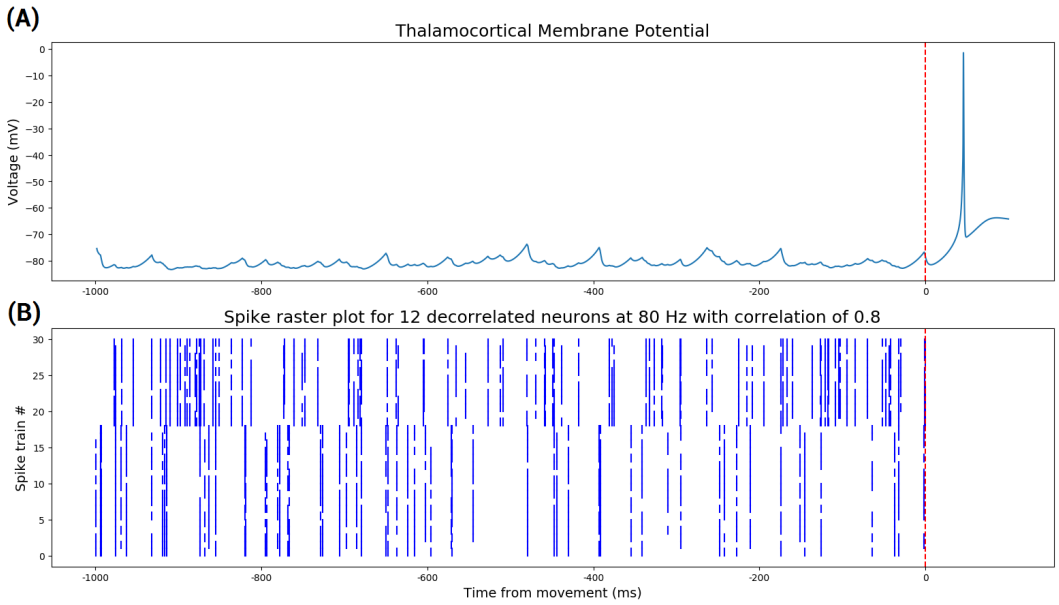

Figure 5. *Spike raster plot and thalamocortical membrane potential for decorrelation simulation.* The simulation parameters for the data seen in this figure are the same as in figure 4. (A) Membrane potential of the thalamocortical neuron. The dashed red line represents the movement onset, where the only rebound spike can be observed. (B) Input SNr spike trains to the thalamocortical neurons. The first 18 spike trains remain at baseline 50 Hz while the last 12 neurons have a firing rate of 80 Hz. Both groups of spiketrains have a correlation of 0.8 within their corresponding groups. There were no pauses greater than 35 ms which induced no unintended rebound spikes

Plotting the spiketrains of the simulated SNr neurons shows much more clearly how both groups emanate from different stochastic processes and how each group of neurons is correlated independently. Both groups complement each other in such a way that it is more difficult to find a pause in the SNr activity, since the pauses in one group are filled with the spikes from the other. A notable example can be seen from -600 to -400 ms, where the group of 18 neurons that fires at baseline 50 Hz has many stops in its activity occupied by spikes from the group of 12 neurons at 80 Hz, stopping possible rebound spikes.

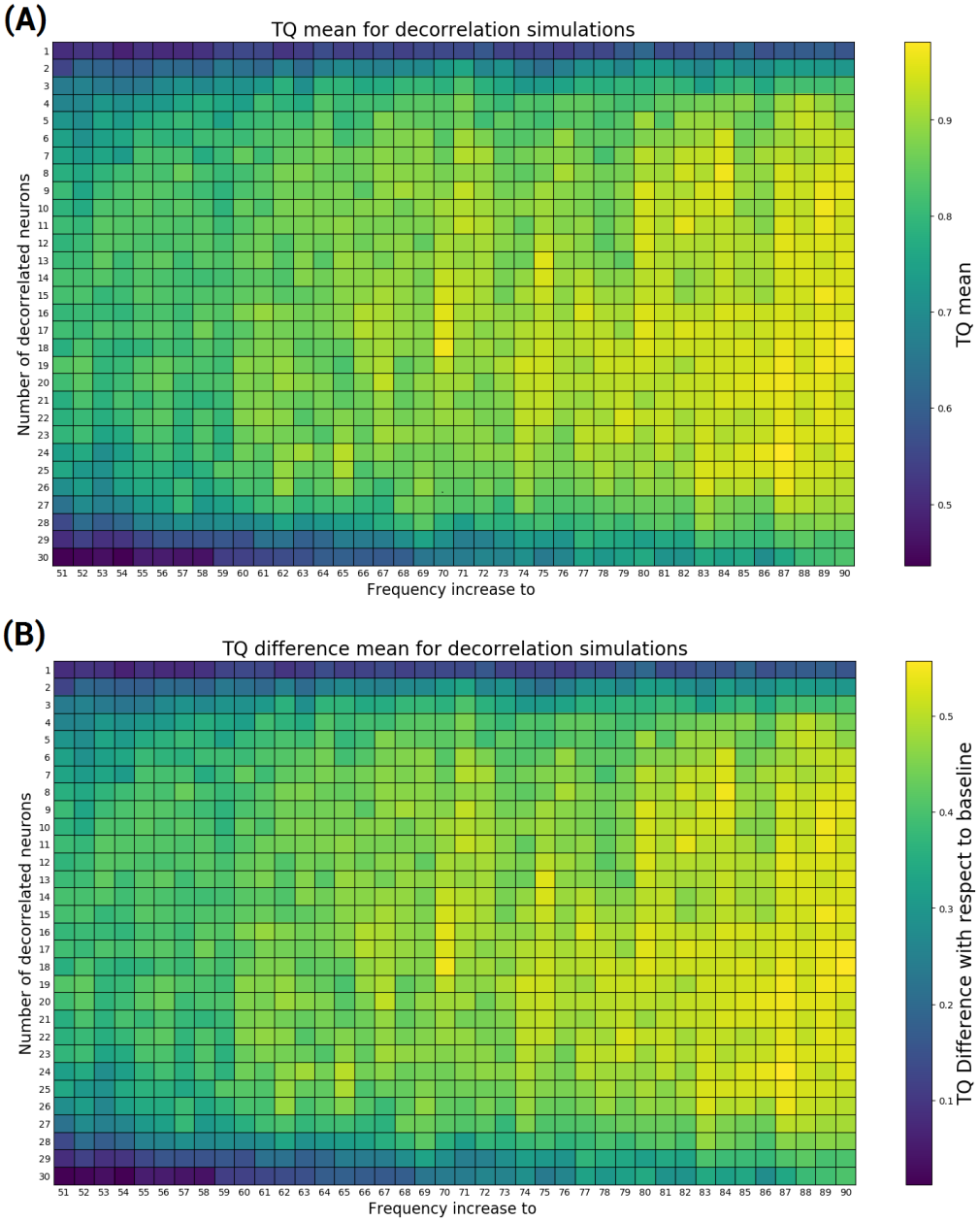

Figure 6. *Transmission quality results for decorrelation simulations.*(A) For every combination of "firing rate increase" and "number of neurons affected" a graph such as figure 3 is generated. If one takes into account that simulations have TQ data for different correlations (figure 3), one could classify the data as 4-dimensional (TQ, correlation, firing rate and number of neurons affected) which would be difficult to show in a single graph in a comprehensible manner. In order to solve this, the data was averaged by correlation, meaning that each square here corresponds to the average of all the correlation TQ results for their specific combination of parameters (TQ results are summed for corr 0.3 to 1 and averaged to obtain the mean). (B) Transmission quality difference with respect to baseline, obtained by subtracting (A)'s results with the baseline scenario with no DBS (30 SNr neurons at 50 Hz).

Looking at the overall transmission quality results across all possible parameter combinations (figure 6) we find interesting results: the transmission quality not only increases when the firing rate increases, but it also increases when the firing rate is fixed and the number of neurons changes.

If the number of neurons parameter is fixed (looking at figures 6A and 6B row-wise) we can observe increases in TQ of 0.4-0.5 from 51 to 90 Hz (6A). It it also quite noticeable how only an increase to 51 Hz can have transmission quality differences of 0.3-0.4 with respect to the baseline no-DBS scenario(6B).

On the other hand, if we fix the frequency increase (looking at figures 6A and 6B column-wise) we can observe an increase in TQ until the number of neurons affected reaches 15, and then promptly drops, following an inverse 'U' distribution. It is also quite relevant how a small number of neurons increased increases the TQ by a considerable amount. In figure 6A the TQ when the number of neurons affected is 1 compared to 5 is quite sizeable, while if we difference in later neurons (for example, from 10 to 15) is not as noticeable.

As explained previously, the correlation of all 30 spiketrains varies substantially from the intended correlation set as the simulation parameter because the correlation between the groups of neurons who were not affected and remain at baseline 50 Hz and the groups of neurons who have been decorrelated with their firing rate increases is practically zero (figure 4).

As a result, the difference between the intended correlation and the correlation obtained peaks when the number of decorrelated neurons and neurons that remain at baseline are both 15 (figure 7A). For all simulation correlation parameters (0.3 to 1), the resulting correlation has a drop of up to 50% (figure 7B) when the number of decorrelated neurons is dropping from 1 to 15, but increases again when the number of affected neurons increases from 15 to 30. The changes seen in decorrelation in figures 7A and 7B, which is similar to the TQ values seen in figure 6 when the firing rate is fixed, are the same for all firing rate increases (Figures 7A and 7B only show correlation changes for firing rate increase to 65 Hz).

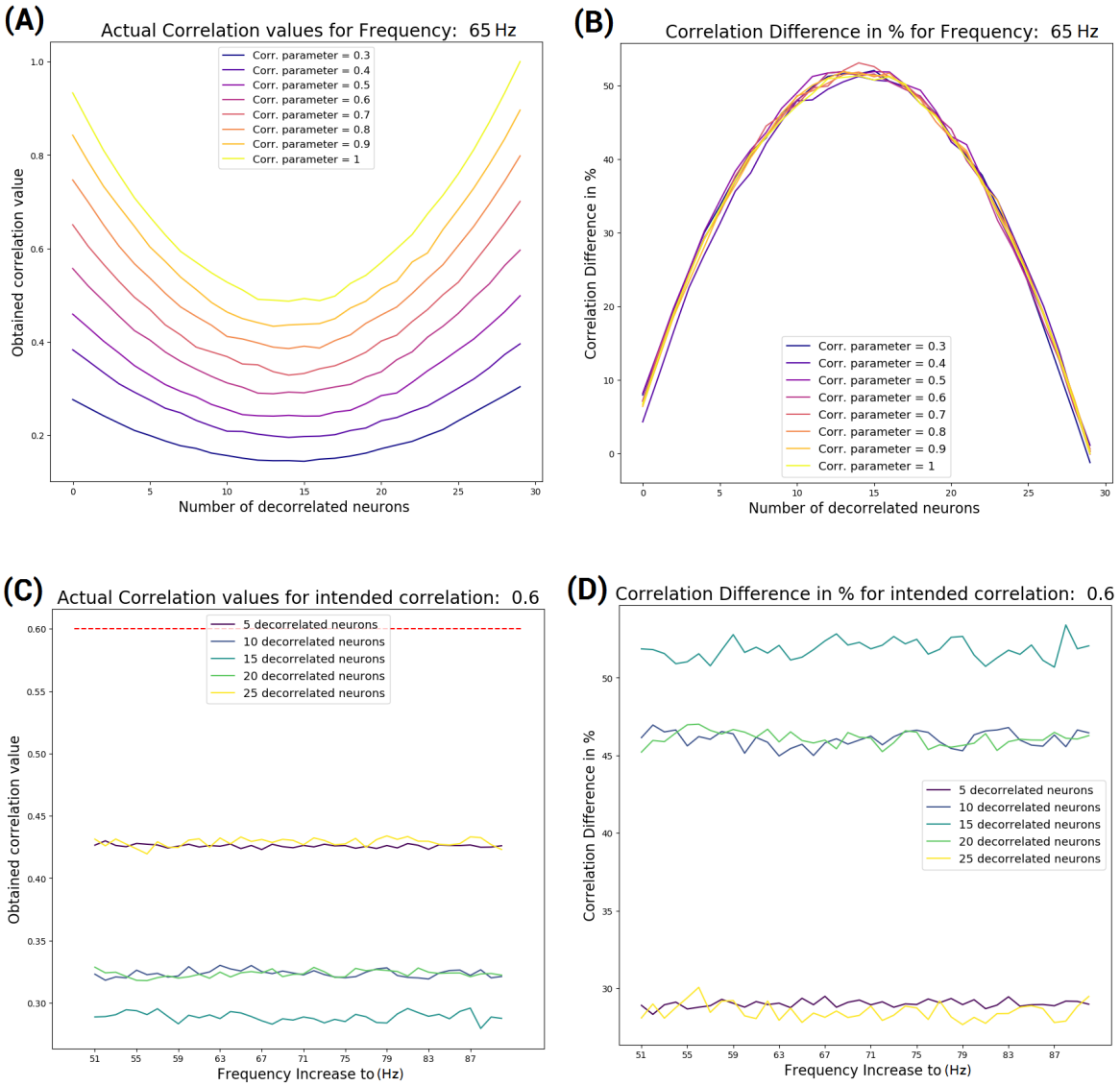

Figure 7. *Correlation study for decorrelation simulations.* The correlation values presented in these graphs are the means of all correlations, as indicated in figure 4. (A) Correlation values obtained for frequency increase to 65 Hz and number of neurons decorrelated for all different correlation parameters. The coloured lines represent the correlation values obtained for each correlation value parameter. (B) Difference in % comparing the correlation simulation parameter and the obtained correlation in figure 7A. (C) Correlation values obtained when the correlation was set to 0.6 across all frequency increases for different numbers of decorrelated neurons. The coloured lines represent the number of decorrelated neurons. The dashed red line represents the correlation parameter used in the simulation (0.6). (D) Difference in % comparing the correlation simulation parameter with obtained correlation values in figure 7C.

Both the correlation and the transmission quality have a significant change when the frequency increase is fixed, but the same cannot be said when the number of decorrelated neurons are fixed. Figures 7C and 7D show that even though the TQ changes as the firing rate increases, the correlation does not. Even though the obtain correlation values differ from the correlation value set as a simulation parameter (figure 7C), the obtained correlation values do not change. The correlation difference is at its peak when the number of neurons from both baseline and decorrelated neurons are 15, but the correlation values remain constant. The results shown in figures 7C and 7D correspond to a fixed correlation of 0.6 for 5,10,15,20 and 25 decorrelated neurons, but the differences in percentages are the same for all different correlation parameters (0.3 to 0.5 and 0.7 to 1).

3.2 A lack of decorrelation in DBS affects transmission quality

For this simulation, the neurons affected by DBS were not decorrelated, and only had their firing rate increased, as explained in section 2.3. This meant that one group of neurons would remain at baseline frequency of 50 Hz and the group of neurons affected by the DBS would have its firing rate increased, with no decorrelation of any kind.

In this simulation, despite having two separate groups of neurons, they both originated from the same stochastic process, the same ”mother spike”, so all neurons shared same degree of correlation. In the simulations where DBS decorrelated the affected neurons, such neurons were not correlated with the neurons who remained at baseline, and thus, both groups had a correlation of 0 when compared against the other, but for this simulation, the correlations between neurons from different groups were not 0(figure 8), which meant the the overall correlation of all spiketrains are higher in this simulation.

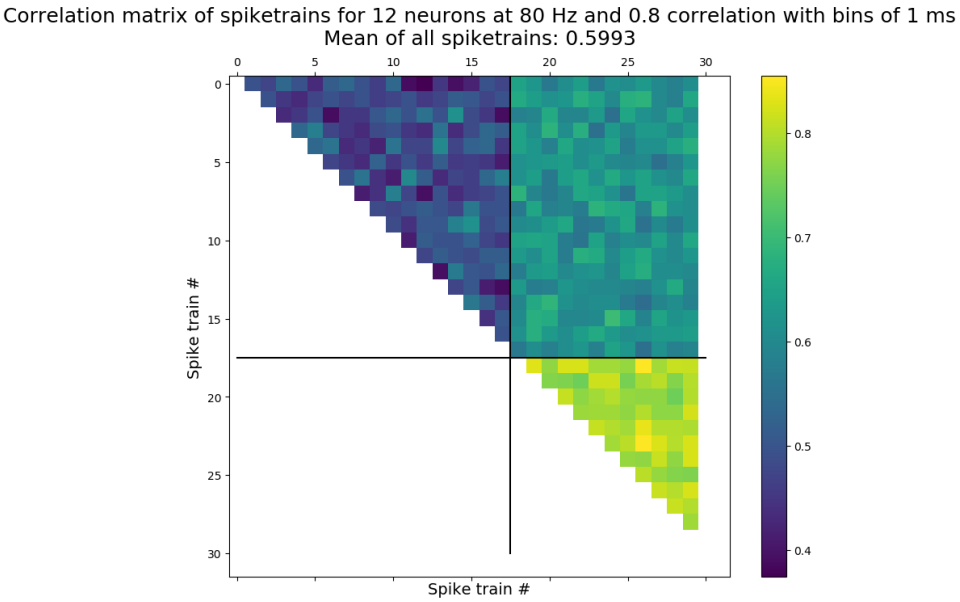

Figure 8. *Correlation matrix for 12 neurons affected by DBS at 80 Hz.* Correlation values range from 0 to 1. As in figure 4, the black lines separate the different groups of neurons. The top left quadrant corresponds to the group of neurons who remain at baseline, while the bottom right quadrant corresponds to the group of neurons that has been affected by DBS and its firing rate increased. Top right quadrant denotes correlation between the neurons of the two different groups. Bins of 1 ms were used for the correlation matrix, and the correlation for this experiment was 0.8. The ”mean of all spiketrains” is calculated as indicated in figure 4.

Figure 8 shows how the correlation is approximately 0.6, when the correlation parameter was set at 0.8. The group of neurons affected by DBS has an average correlation of 0.8, which was the parameter for this specific simulation, but the group of neurons who remained at baseline has an average correlation of 0.48. This difference in correlation with respect to 0.8 originates from the process via which the 50 Hz baseline spike trains are created, as explained in section 2.3.

Furthermore, the correlation between the spiketrains of the two different group of neurons is 0.62, a noticeable difference compared to the simulation where DBS decorrelated the affected group of neurons (figure 4), where such correlation between both groups was 0. The correlation between both groups can be understood when one takes into account that both groups of spiketrains are multiple-interaction processes that originate from the same ”mother spike train”, meaning that both groups will be correlated.

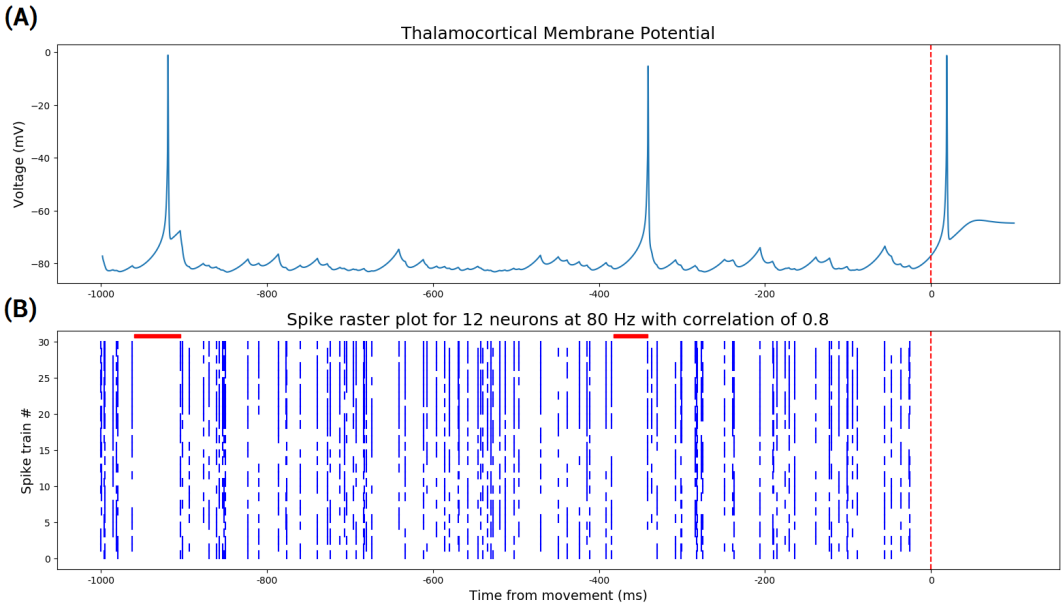

Figure 9. *Spike raster plot and thalamocortical membrane potential for DBS without decorrelation*. The simulation parameters for the data seen in this figure are the same as in figure 8. (A) Membrane potential of the thalamocortical neuron. The dashed red line represents the movement onset. There are 2 rebound spikes before the movement onset. (B) Input SNr spike trains to the thalamocortical neurons. The first 18 spike trains remain at baseline 50 Hz while the last 12 neurons have a firing rate of 80 Hz. The red rectangles on the top of the raster plot denote pauses of more than 35 ms, which are capable of eliciting rebound spikes, which they both did.

Comparing these spiketrains of figure 9B to figure 5B helps shows how all spiketrains originate from the same stochastic process and how the group of neurons affected by DBS is not decorrelated. In this situation the pauses are more frequent and longer than in figure 5B, eliciting 2 rebound spikes. This difference between the simulations described in 3.1 and this section are most notable for low frequency increases, where the transmission quality in the simulations described in this section are lower compared to the simulations described in section 3.1.

Moreover, the overall transmission quality results for all simulations (figure 10), not only shows a substantial difference in TQ in lower frequencies compared to figure 6, but a different pattern as well: transmission quality does not vary when the number of neurons affected by DBS changes but it still increases when the fire rates does so as well.

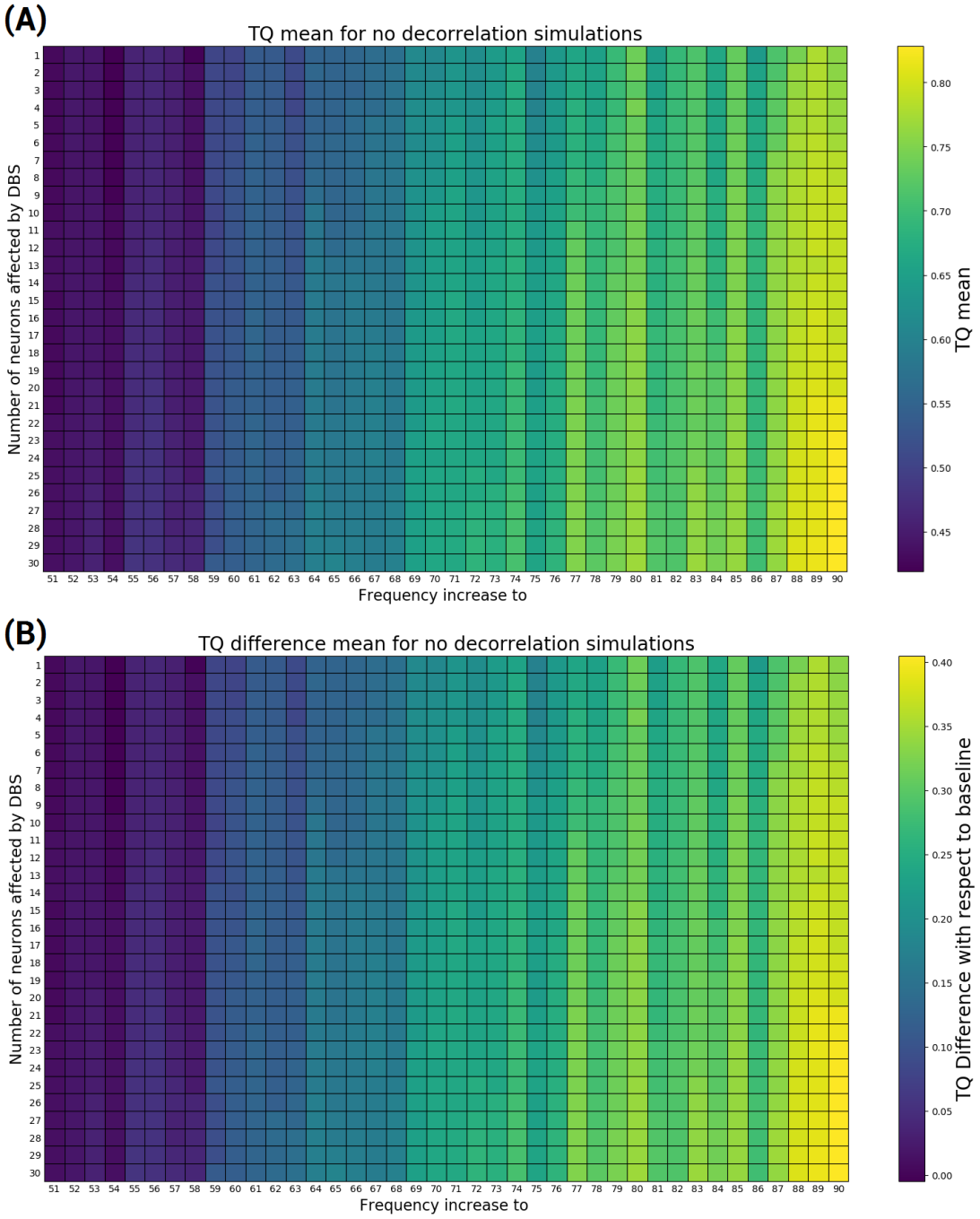

Figure 10. *Transmission quality results for simulations with no decorrelation.*(A) Data plotting followed the same process as described in Figure 6A. TQ was also performed for correlation parameters 0.3 to 1. (B) Transmission quality difference with respect to baseline, obtained by subtracting (A)'s results with the baseline scenario.

The transmission quality for low frequency increases (51-60 Hz) is quite low (figure 10A) in comparison to the TQ where neurons affected by DBS are decorrelated (figure 6). The TQ results are so low for these low frequencies, that they sometimes do not even improve the TQ at all (figure 10B).

Nonetheless, as also seen in figure 6A, the TQ increases when the firing rate increases. If the number of neurons increased by DBS is fixed, and we only look at the results row-wise, increases of TQ by 0.25-0-35 can be appreciated (10A).

However the same cannot be said for the number of neurons affected by DBS. Increasing the number of neurons affected by DBS does not have very noticeable changes in comparison to figure 6A. Fixing the frequency increase and looking at 10A and 10B column-wise shows that the TQ sometimes does not change at all or very little (Frequency increases to 51-70 Hz. For higher frequency increases such as 77, 83 or 88-90 Hz, the TQ does increase, albeit not on a very big scale if compared to figures 6A and 6B.

The correlation results from the simulations (figure 11) also differ substantially from the ones obtained in section 3.1 (figure 7). The difference lies in the correlation matrix of figure 8, since correlation between spiketrains- for simulations where the DBS does not decorrelate the affected neurons is different when the DBS does decorrelate such neurons (figure 4).

Figures 11A and 11B show that as the number of neurons increase for 65 Hz, the correlation values increase in a linear fashion. For all correlation parameter values, the increase in correlation percentage is the same (figure 11B), and the lowest correlations correspond to the lowest number of neurons affected by DBS. As the frequency increases, the obtained correlation values still maintain a linear progression, but with a larger slope. For 65 Hz, the correlation difference starts at 23% approximately for 1 neuron and decreases to 0%. For 90 Hz, the difference starts at 42% and decreases to 0%. This implies that for all frequency increases, all obtained correlations increase as the number of neurons increases, where as the maximum number of neurons affected by DBS is reached (N = 30), the correlation obtained equates the correlation set as a simulation parameter.

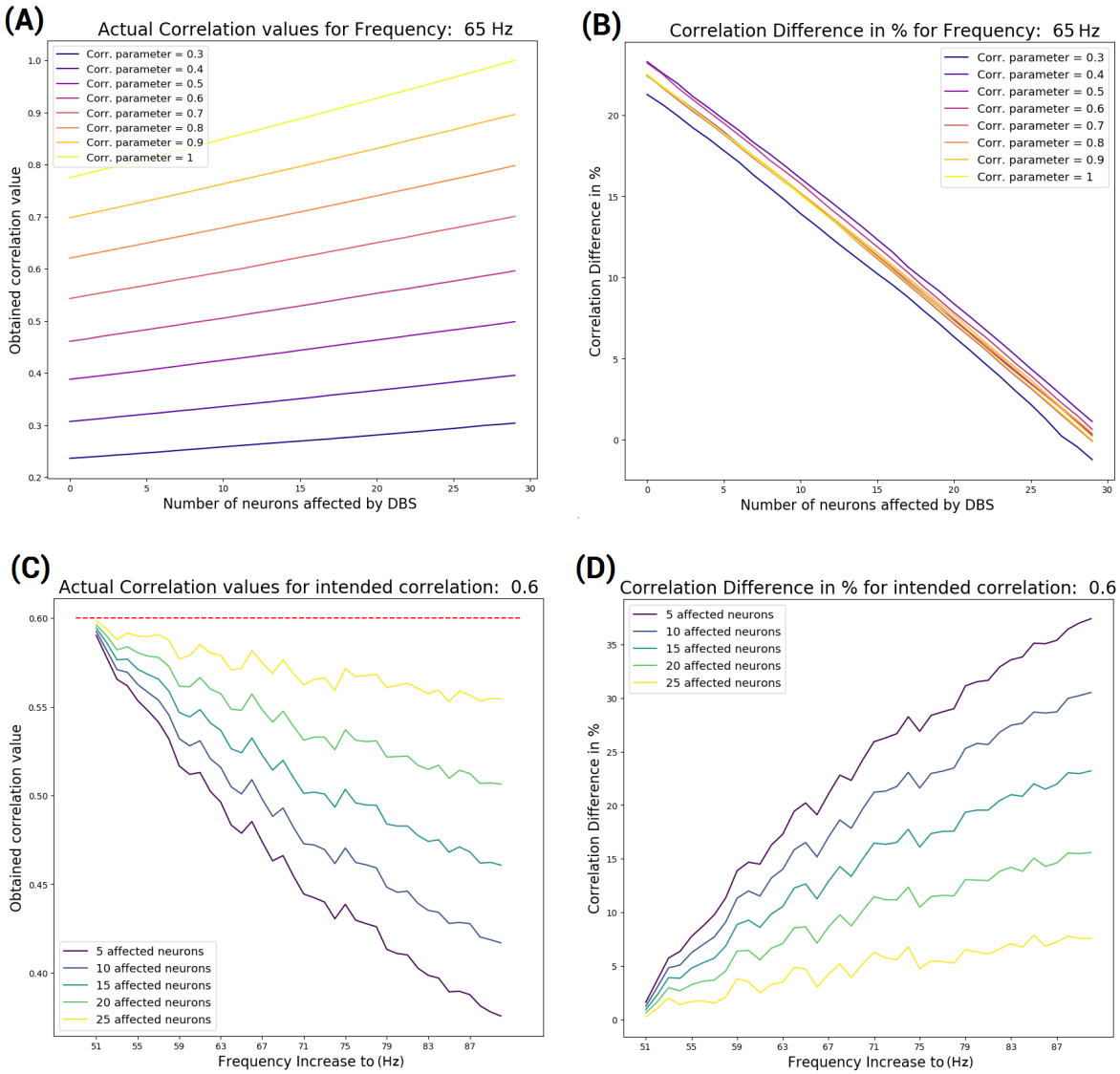

Figure 11. *Correlation study for simulations with no decorrelation.* The correlation values presented in these graphs are the means of all correlations, as indicated in figure 8. (A) Correlation values obtained for frequency increase to 65 Hz and number of neurons affected by DBS for all different correlation parameters. (B) Difference in % comparing the correlation simulation parameter and the obtained correlation in figure 11A. (C) Correlation values obtained when the correlation was set to 0.6 across all frequency increases for different numbers of neurons affected by DBS. The coloured lines represent the number of neurons affected by DBS. The dashed red line represents the correlation parameter used in the simulation (0.6). (D) Difference in % comparing the correlation simulation parameter with obtained correlation values in figure 11C.

Figures 11C and 11D show correlation results when the numbers of neurons are fixed. In these simulations, as the firing rate increases, the correlation decreases. The lower the number of neurons affected by DBS, the lower the correlation (11C). The difference in % values obtained in 11D are the same for all correlation value parameters, as in section 3.1.

3.3 Transmission quality differences using biological data

In section 1.1, deep brain stimulation wash shown to have a very heterogeneous effect, as it can affect groups of neurons independently and correspondingly increase or decrease their firing rate. At the same time, some neurons are not affected by the DBS and remain at their corresponding firing rate as well[9].

To illustrate the importance of decorrelation and the role it plays in transmission quality, we will use Hahn's study and use the biological data from the GPi he obtained from a rhesus monkey that underwent DBS and use it in our two different simulations described in sections 3.1 and 3.2.

The data obtained from Hahn's study was described in figures 2B1 and 2C1. Figure 2B1 showed the frequency increases and decreases during DBS, while figure 2C1 showed the percentage of neurons that were not affected by the DBS, the percentage that had its firing rate increased and the percentage that had its firing rate decreased.

11% had no significant change in its firing rate, which was calculated as a group of 3 neurons that were not affected by DBS and thus remained at 50 Hz. 32% of neurons had a decrease of firing rate, which was translated to a group of 9 neurons that had its firing rate decreased to 20 Hz. Lastly, 58% of neurons had its firing rate increased, meaning that the remaining 18 neurons had their frequency increased to 82 Hz.

In order to simulate DBS with decorrelation, all 3 groups of neurons were decorrelated, meaning that as explained in section 2.3, all 3 groups generated their corresponding mother spiketrain and drew spikes from it. On the other hand, to simulate DBS with no decorrelation, a process similar to section 2.3 was used: All 30 spiketrains were drawn from a single mother spiketrain and generated with a firing rate of 82 Hz (the highest among the 3 groups), and for each corresponding group, random spikes were

deleted in order to have two groups of 50 and 20 Hz respectively. All simulations had 100 trials since the simulations were not computationally expensive.

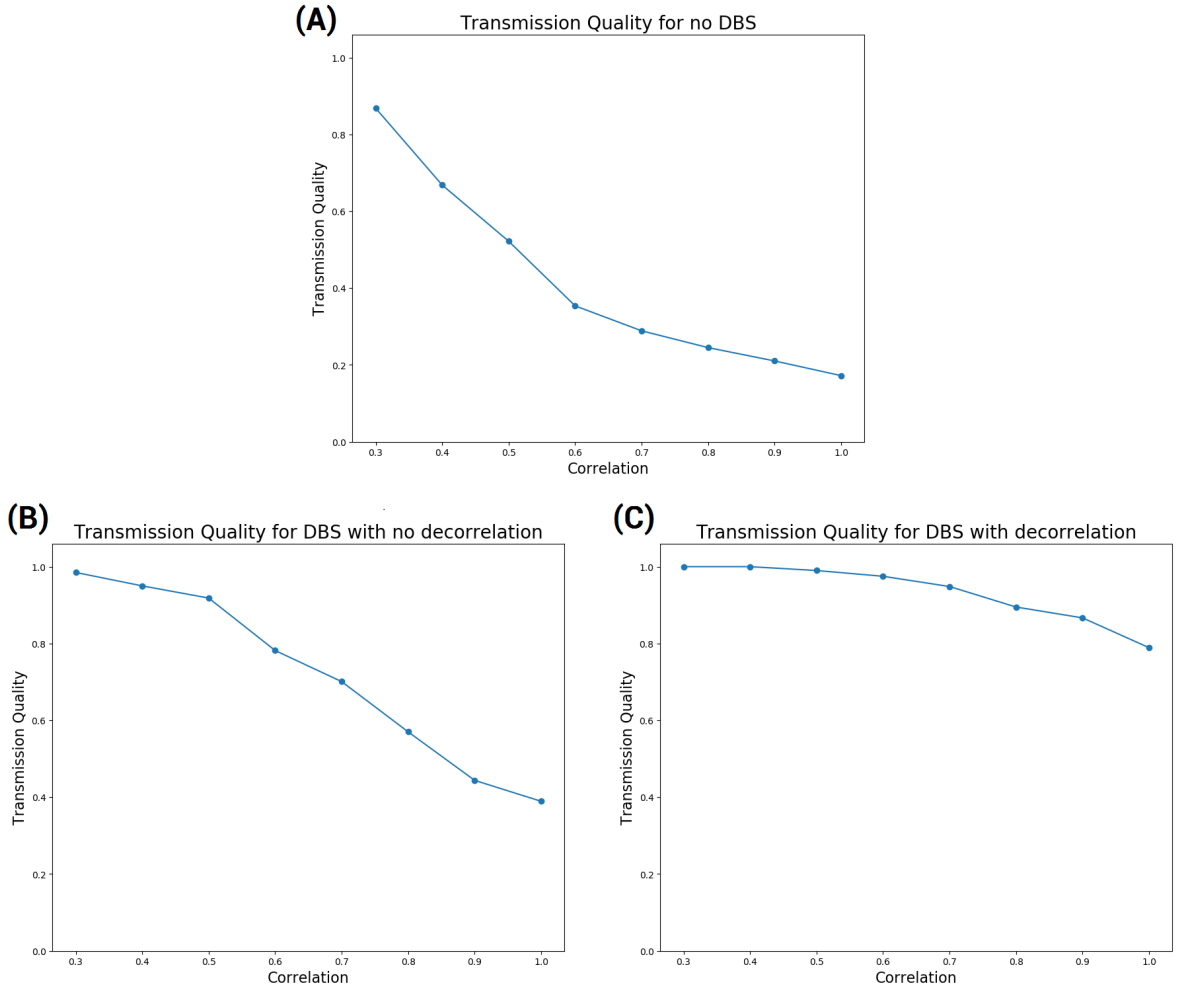

Figure 12. *Transmission quality results for simulations with biological data from Hahn's study.* (A) Baseline scenario where no DBS is applied, 30 neurons at 50 Hz for degrees of correlation from 0.3 to 1. (B) TQ results for DBS simulations with no decorrelation for the affected groups of neurons. (C) TQ results for DBS simulations with decorrelation for the affected groups of neurons.

295 The transmission quality from the two different methods of DBS show a clear difference in efficacy. While Figure 12B shows that there is a noticeable increase in TQ when it is compared to figure 12A for correlations of 0.3-0.6, it drops off quickly for the latter values. On the other hand, the decorrelation simulations in figure 12C see a much greater improvement in TQ, where the lowest TQ is 0.7892 for a

correlation of 1. Both methods of DBS bring an improvement in TQ, but the decorrelation simulations clearly show a bigger benefit in TQ.

3.4 Having small fixed groups of decorrelated neurons increases transmission quality

As seen in section 3.1, 3.2 and 3.3, the effect of decorrelation is quite significant in terms of transmission quality. Since section 3.2 showed results for neurons who were not decorrelated by DBS, and in section 3.1 all neurons who were affected by DBS were decorrelated, another set of simulations were performed, were DBS would only decorrelate a small group of neurons.

Such simulations were primarily based on section 3.2, where the number of neurons affected by DBS were not decorrelated, but the the simulation parameter of ”number of neurons affected by DBS” would not vary from 1 to 30. Instead, the number would go from 1 to 30-X, where X is the fixed amount of decorrelated neurons. As an example, if the fixed amount of decorrelated neurons is 5, in a simulation where the number of neurons affected by DBS is 10 and the corresponding frequency increase is to 80 Hz, the following spiketrains would be generated:

- 17 spiketrains unaffected by DBS who remain at 50 Hz
- 10 spiketrains affected by DBS who have their firing rate increased to 80 Hz
- 3 spiketrains decorrelated by DBS who have their firing rate increased to 80 Hz

Based on figure 6, a small group of decorrelated neurons had a big impact on transmission quality, so simulations for 1 to 5 fixed decorrelated neurons were performed. As the number of decorrelated neurons increased from 1 to 5, the corresponding TQ results improved in a linear fashion. While the results were not as different as if we compared section 3.2 to 3.1, the differences were still quite significant.

The results shown in this section will correspond to a fixed group of 3 decorrelated neurons. The parameters used in this simulation were the same as in sections 3.1 and 3.2, with the exception of the ”number of neurons affected by DBS”, which ranged from 1 to 27, instead of 1 to 30, as explained previously.

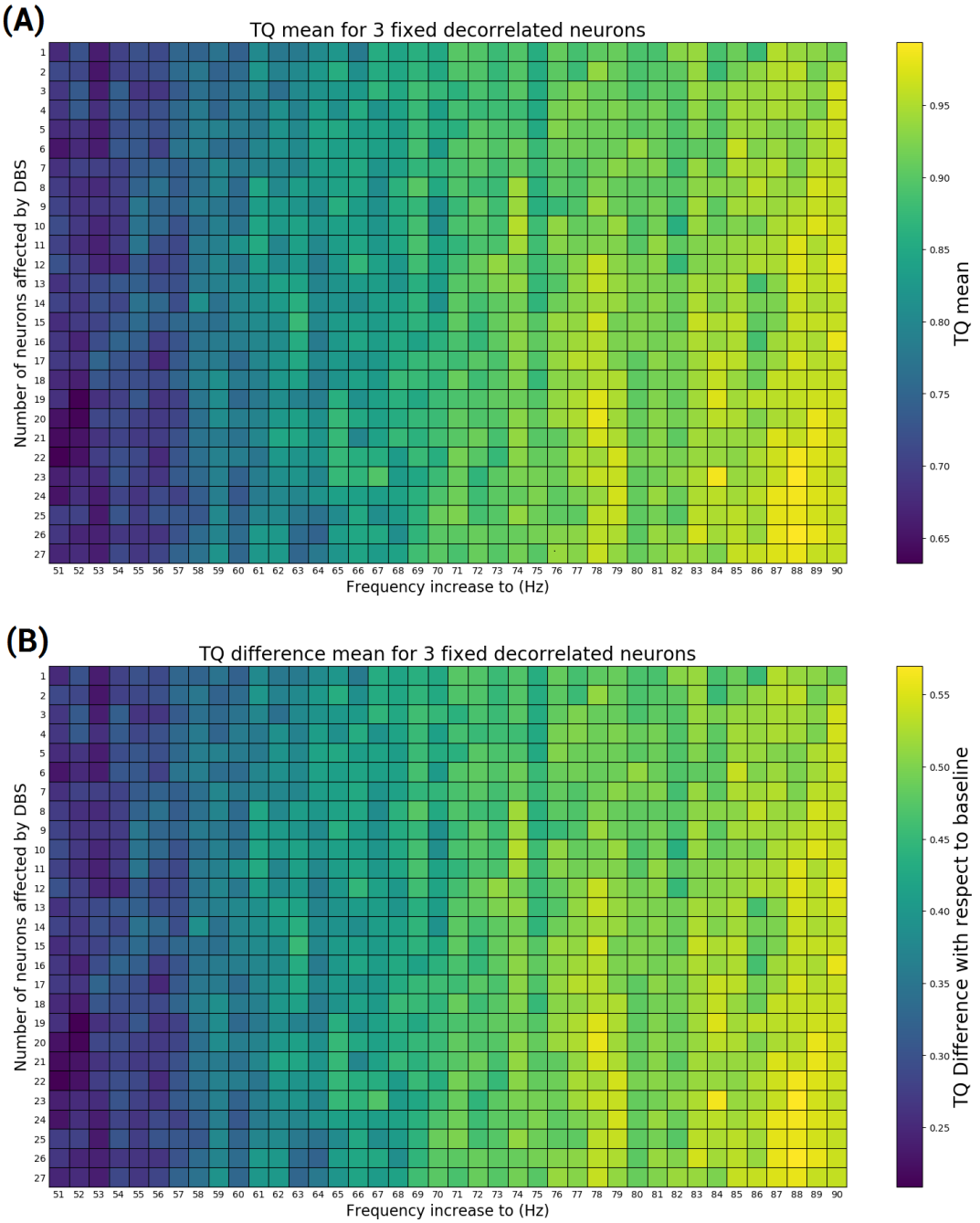

Figure 13. *Transmission quality results for simulations with 3 decorrelated neurons.*(A) Data plotting followed the same process as described in Figure 6A and 10A. The number of neurons affected by DBS (Y axis) ranges from 1 to 27. All simulations include a fixed group of 3 decorrelated neurons with their corresponding firing rate increase. (B) Transmission quality difference with respect to baseline, obtained by subtracting (A)'s results with the baseline scenario.

The benefits of having 3 correlated spiketrains are quite substantial. Figure 13A shows that for firing rates of 70 Hz and higher the TQ is over 0.9. While the lower firing rates yield lower transmission qualities, figure 13B reveals that they still improve TQ by 0.2-0.25. Figure 10B showed that for low firing rates the TQ increase was very low , ranging from 0 to 0.1, while Figure 13B shows that the lowest increase is approximately 0.2.

The pattern seen in figure 13B shows that TQ increases in a linear fashion as firing rate increases, albeit with higher values and a higher slope compared to figures 6A and 10A. There are also TQ changes as the number of neurons affected by DBS increases, but a clear pattern cannot be seen in such changes, who are often in the range of 0.05.

The transmission quality was not the only change seen in this simulation: the resulting correlations for all 30 spiketrains during DBS also had relevant changes. Figure 14 shows similar results to Figure 11, but on a different scale. The correlation obtained during DBS shows the same behaviour as in section 3.2, but the values were lower. Figures 14B and 14D not only show how the correlation pattern is very similar when compared to figures 11B and 11D, but also that the correlation is lower by a factor of 17.5% (figure 14B) and 10% (figure 14D). The result of having 3 decorrelated neurons seems to lower the correlation values, since this decrease was persistent across all firing rate increases and all correlation simulation parameters.

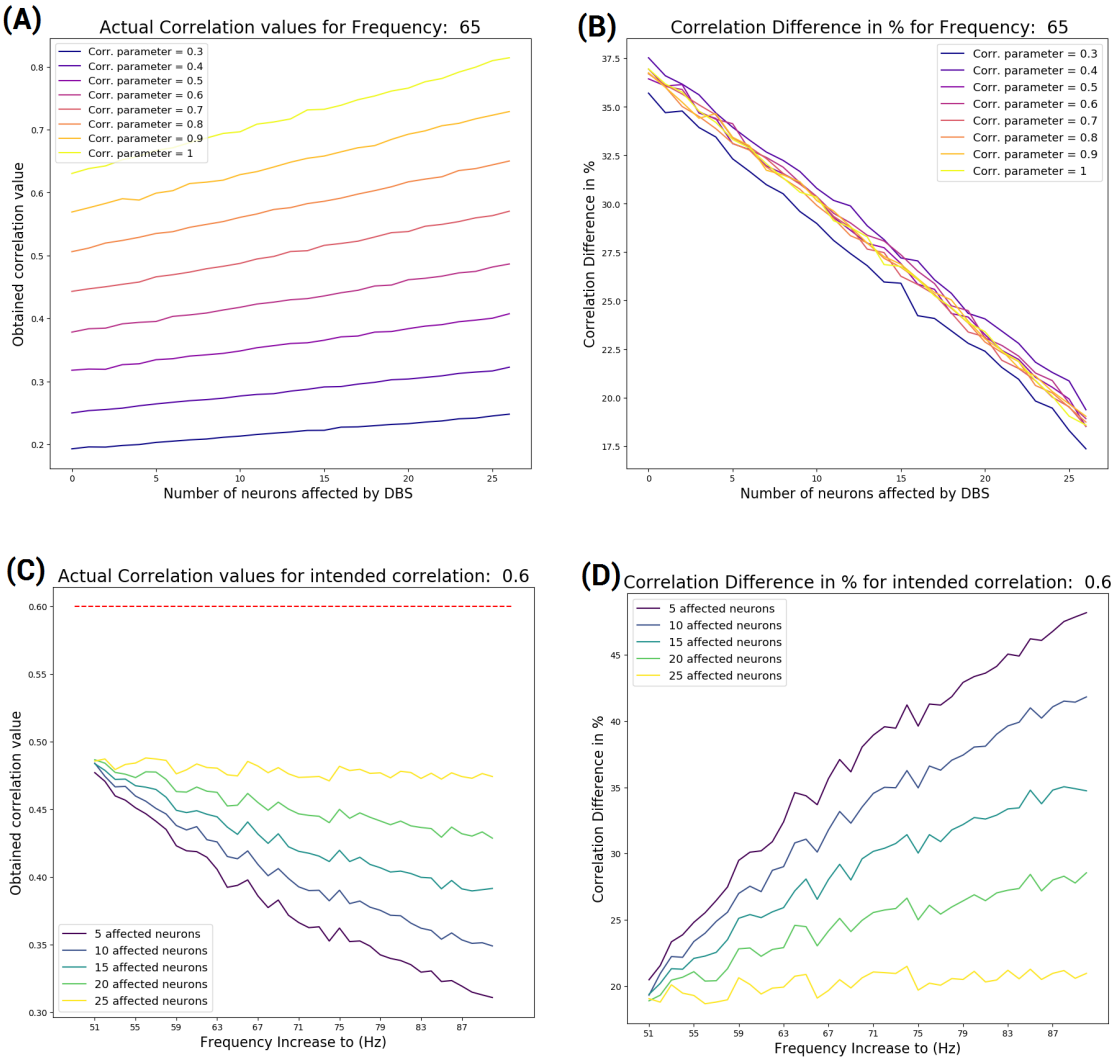

Figure 14. *Correlation study for simulations with 3 decorrelated neurons.* Correlation values shown follow were calculated the same way as in figure 7 and 11. (A) and (C) have the same description as 11A and 11C. (B) Difference in % comparing the correlation simulation parameter and the obtained correlation in figure 14A. (D) Difference in % comparing the correlation simulation parameter with obtained correlation values in figure 14C.

4 Discussion

Taking into account how DBS has been shown to have a heterogeneous effect and have limited efficacy on some individuals[9][10], the simulations presented in section 3 were of a very simplistic nature compared to its actual biological effects.

Nevertheless, the simulations were purposely designed in such way, so that it would be easier to understand the results and perform the corresponding data analysis and to show how such simplistic simulations are capable of yielding meaningful results. Sections 3.1, 3.2 and 3.4 had only one group of neurons affected DBS with a firing rate increase, and biological data show that several groups of neurons have both increases and decreases for different firing rates, with groups of neurons not affected by the DBS.

However, even if the simulations were very different and could be classified as simplistic, the results showed how variations in such simulations yielded very different results: not only were the TQ results very different from each different simulation and varied significantly for different simulation parameters, but the correlation during DBS also showed different patterns depending on the type of simulation and on the corresponding simulation parameters.

Section 3.3 used biological data and performed simulations for a specific set of parameters to show the importance of decorrelation. While the exact benefit of performing many additional simulations such as having three groups instead of two (with varying simulation parameters as sections 3.1, 3.2 and 3.4), having not only firing rate increases but also decreases, etc. could give additional insights, the objective of this study was to demonstrate the study the variation of correlation/decorrelation for DBS and to show its importance.

4.1 The effect of deep brain stimulation on correlation and transmission quality

The simulations in which DBS decorrelated all neurons that it affected (section 3.1) showed quite significant results in terms of transmission quality and correlation. The increase of TQ as the firing rate increased were not particularly outstanding (figure 6A), since an increase in firing rate leads to a lesser possibility of pauses. However, the increase of TQ when the number of decorrelated neurons increased

for a set firing rate was more striking.

Having only 3-5 decorrelated neurons improved the TQ significantly, and as one crossed the 15 decorrelated neuron mark, the TQ results worsened. This could be explained by figure 5, which shows that as the number of decorrelated neurons approached 30, the effect of having two groups of decorrelated neurons who fill each other's gap in activity is decreased. However, the changes in correlation during DBS (figure 7) help understand such changes in TQ.

Figures 7C and 7D show how despite there is a change in correlation during DBS, but such change does not increase or decrease for higher firing rates, and instead remains in a straight linear fashion. The lack of such change for increases in firing rate shows that there is no specific need for changes in decorrelation for improvements in TQ when the firing rate increases. However, figure 7D shows that 15 decorrelated neurons have the biggest decrease in correlation during DBS, showing a correlation between the TQ values shown in figure 6.

On the other hand, figures 7A and 7B do show a pattern in correlation values during DBS when the number of decorrelated neurons changes. Figure 7B shows the same pattern as the TQ in figure 6A, where the maximum decrease in decorrelation during DBS is achieved when the number of decorrelated neurons is 15, and the correlation increases in both directions after that. Still, with only 5 decorrelated neurons, we can see a decrease of over 30%, which is quite significant and shows the impact that a small group of decorrelated neurons has. Additionally, Figure 7A shows how that the extremes (1 and 30 decorrelated neurons) obtain the worst TQ results, since they are not capable of reducing the correlation, and the correlation during DBS remains as it was in its pathological state.

Figure 15 in appendix 1 show all of the simulation results in two different scatterplots, and they both reinforce that firing rate and correlation play a role in TQ. Figure 15A shows an easily observable correlation between TQ and correlation during DBS: the lower the correlation, the higher the TQ. Likewise, figure 15B shows correlation between TQ and the firing rate increase, but not as substantial as figure 15A, revealing how much of an impact the correlation has on TQ.

For the DBS simulations where the neurons are not decorrelated, the results in both TQ and correlation

are different. As expected, figure 10 shows how the higher the firing rate of the neurons affected by DBS, the higher the TQ, but increasing the number of neurons affected by DBS does not seem to assure an increase in TQ. The slight increases in TQ when the number of neurons is higher for some frequencies may be a byproduct of the stochastic nature of the simulations, and isn't too significant. It is worth mentioning how the increase in TQ due to firing rate can reach differences of 0.35-0.4 when comparing both ends of the firing rate increases (51 to 90 Hz), a bigger difference compared to its decorrelation simulation counterpart.

In this case, figures 11C and 11D do show a decrease in correlation during DBS as the firing rate increases. Such decreases in correlation appear to be linear, and since section 3.1 did not show such changes, these linear decreases in correlation could explain why the TQ increases are more notable compared to section 3.1. These figures also reinforce the notion that TQ increases with higher firing rates, with or without changes in correlation. The corresponding scatterplot for TQ and firing rate increase (figure 16B) shows a slightly stronger correlation than figure 15B, which showed the same scatterplot but for DBS with decorrelation.

Figures 11A and 11B showed quite different results in comparison to figures 7A and 7B. Not only does the decorrelation increase change in a linear fashion as the number of neurons affected by DBS increases, the overall values are also lower (figure 11B). These results are quite relevant, since despite there being no apparent change in TQ with different number of neurons affected by DBS, correlation values during DBS do change. The difference in correlation for both simulations is very different: DBS with decorrelation (figures 7A and 7B) show a parabolic distribution of correlation values, while DBS without decorrelation (figures 11A and 11B) show a linear increase in correlation as the number of affected neurons grow larger. It can be inferred that there is a non-linear relationship between correlation and TQ when firing rate and other possible physiological factors are not taken into account.

As a result of DBS with no decorrelation not being as efficient in lowering its correlation as its counterpart with decorrelation, figure 16A in appendix 2 shows how there many more results where correlation was lower compared to figure 15A of appendix 1 (DBS with decorrelation). Nevertheless figure 16A also

show a clear linear relationship between correlation and TQ. Despite DBS with and without decorrelation yielding very different TQ and correlation results, they both indicate that there is a relationship between correlation and TQ, and that the desirable outcome for simulations is to have its correlation reduced as much as possible.

Overall, both simulations did reduce the correlation during DBS, albeit with different efficacy, and as a consequence, the TQ improved for both scenarios. However, the decorrelation of groups of neurons showed that even a small group of neurons can bring quite significant improvements in TQ, since they brought the overall correlation of all 30 neurons down quite significantly, even with as few as 3-5 decorrelated neurons. Looking at figures 6A and 10A for a firing rate increase to 51 Hz shows how much of an impact decorrelation has.

As it was explained in the beginning of this section, these simulations are very simplistic in nature, but are still capable of giving powerful insights. Section 3.3 showed how more complex simulations, which are in theory closer to their biological counterpart, give very different results only by having neurons decorrelate or not.

However, even if sections 3.1 and 3.2 were simplistic simulations, they could be thought of as ”counterparts”, where section 3.1 decorrelated every neuron that it affected, while section 3.2 did not have any decorrelation. While it sounds too optimistic for DBS to decorrelate every single neurons, it could also be argued that it is also quite pessimistic to assume that DBS would not perform no decorrelation at all, as in section 3.2.

As discussed previously, decorrelation can be very impactful even if only a small group of neurons is affected by it. In order to both perform simulations that are not either too ”pessimistic” or ”optimistic” and to show the effect a small group of decorrelated neurons has, simulations as indicated in section 3.4 were performed. In such simulations 1 to 5 neurons were always decorrelated, and as the number of decorrelated neurons increases, so did the TQ results (figure 13), and the correlation during DBS was lower as well (figure 14).

The simulations shown on section had 3 neurons who were always decorrelated with a frequency increase

by DBS, aside from the other neurons that DBS affected, but with no decorrelation. TQ results (figure 13) show how the results still improve as the firing rate is increased, up the the point where the highest firing rates in the simulation have TQ results over 0.9 or more. Figures 14C and 14D show that the correlation during DBS is also lower when compared the the simulations with no decorrelation (Figures 11C and 11D). Likewise, we a change when the number of neurons affected by DBS (with no decorrelation) can be seen, but without a clear pattern. This change can also be explained with figures 14A and 14B, where the linear trend still persists, but with lower correlation values overall. Additionally, we do not see a change in TQ (when the number of neurons affected by DBS varies) as meaningful in the simulations were all neurons affected by DBS were affected (Figure 6), reinforcing the notion that changes in correlation need to be more complex than a linear increase or decrease for such changes to be appreciated.

Having only a small fraction of decorrelated neurons reduces correlation during DBS and correspondingly increases the TQ. Figure 17B in appendix 6.3 shows how increases of firing rate bring better TQ compared to not having any decorrelated neurons (figure 16B, appendix 6.2). Figure 16A also shows how the correlation during DBS is also lower, and showing the corresponding increases in TQ.

Overall, the benefits of having a small group of decorrelated neurons are very clear, since they bring the overall correlation down and increase the TQ. As explained before, these simulations could also be considered simplistic, since they only show a fixed group of decorrelated neurons with a firing rate increase. Additional simulations could include random firing rate increases for decorrelated neurons, firing rate decreases, etc. Despite this, these simulations also show how a small group of decorrelated neurons is very beneficial and should be sought in DBS.

4.2 Changes in correlation and decorrelation induced by deep brain stimulation could explain its efficacy

Deep brain stimulation is also called in the medical filled HF DBS, where HF stands for High Frequency, since it delivers high frequency pulses through its electrodes. It is especially successful in PD patients[6], but the process the effect of DBS on neuronal firing is not well known[19].

Many studies have been performed to understand the effect of DBS in the different regions of the basal ganglia and how they affect properties such as neuronal firing rates, bursting rates, etc. Such studies have reported many different outcomes from the same type of DBS, which eventually led researchers to agree on the heterogeneous effect of DBS. Hahn's work on two rhesus monkeys who were induced with MPTP[9] showed how the effects of DBS on these two subjects were very heterogeneous: several groups of neurons were either affected, with increases and decreases in both firing rate and different bursting types, while other groups of neurons were not affected.

However, Hahn also reported that one monkey showed benefits in motor symptoms despite it did not show relevant changes in firing or burst rate. Hahn attributed this counter-intuitive case to other physiological changes apart from firing rate and bursting, since these two were the objective in his study and he found that they were not enough to account for improvements in PD patients.

We gathered Hahn's results on the monkey that had changes in its firing rate and used them as data for our simulations (section 3.3). In hahn's study, the GPi had 58% of its neurons increase its firing rate, 31% decreased their firing rate and 11% of them were unaffected by the DBS. We calculated the corresponding amounts for our simulations where we used 30 neurons and calculated firing rates according to Hahn's report. We did not have a firing rate for every single neuron, but rather had all neurons fire at the same firing rate, which were 82, 20 and 50 Hz respectively.

The results for this simulation based on biological data showed very different transmission quality results (figure 12). While the simulation where DBS did not decorrelate the neurons it affected showed an increase in TQ, the simulation where DBS did decorrelate the neurons it affected had much higher TQ results.

Both simulations showed the same changes in firing rate, and changes in the coefficient of variation of the interpsike interval were not significant, as in Hahn's study. The only difference between both simulations was the presence of decorrelation in the simulation that yielded better TQ results, which also had lower correlation values for all 30 spiketrains during DBS. For studies, such as Hahn's , were correlation is not a studied variable, one could not be able to understand the efficacy of DBS despite changes in firing rate

for example. If we had a PD patient with an advanced case of PD, which could be simulated by having a pathological SNr correlation of 0.8-1, the effect of DBS with decorrelation vs no decorrelation would be quite significant, and possibly explain the success behind the procedure if decorrelation was achieved.

Animal studies are not the only ones who report cases of ineffective DBS, where 11 to 15& of PD patients do not show improvements in motor symptoms[20]. Correlation and decorrelation should be added in such studies, since they could account for the varying effects of DBS, and ultimately help us understand the effect of DBS.

Alternatively, one could justify that research efforts should not be placed into understanding our current DBS techniques, but rather, to create and/or perfect new types of DBS that actively decorrelate the neurons it affects. After all, HF DBS was developed empirically and based on observations[21]. Hauptmann and Tass proposed a new type of DBS known as Coordinated Reset (CR) stimulation with the objective of restoring segregated neuronal connectivity, which is obtained by decorrelating the pathological correlated state of PD[22]. Their work consisted of a human computational STN-GPe model to study the effect of both HF and CR DBS on the restoration of segregated connectivity

Hauptmann and Tass are interested segregated connectivity because apart from pathological correlation seen in PD patients, PD is also responsible for the loss of such segregation in functional microcircuits[23] due to the death of dopaminergic systems, which maintain such segregation. Hauptmann and Tass' simulations are based on Shink et al's findings, who showed that the interconnections in STN are organised in small local microcircuits[24], which were later shown to process distinct sensory information[25].

Hauptmann and Tass modelled three distinct microcircuits of the STN and simulated HF DBS and CR DBS. For HF DBS, segregation was restored moderately but the pathological synchronised connectivities were not removed. On the other hand, CR DBS successfully restored segregation activity in its microcircuits and effectively reduced pathological synchronisation.

A comparison to sections 3.1 and 3.2 could be made, where DBS with no decorrelation could represent HF DBS, and DBS with decorrelation could represent CR DBS. Both simulations reduce the pathological correlation during DBS, but section 3.1, that is, DBS with decorrelation, is the one who reduced the

correlation the most and as a consequence yielded better TQ results.

CR DBS may be the necessary approach, since it has been demonstrated in such computational models that it restores segregated connectivity and reduces pathological connectivities, which in turn returns the basal ganglia to its healthy uncorrelated state. CR DBS was shown to produce long-term desynchronisation in a hippocampal slice of a rat[26] and a recent study of CR DBS on a MPTP induced primates revelaeed that CR DBS obtained comparable or better motor improvements compared to HF DBS, with longer lasting effects and less stimulation (as predicted in Hauptmann and Tass' model)[27].

The potential superiority of CR DBS over traditional HF DBS due to its focus on restoring segregation and correlation shows the importance of decorrelation. More emphasis needs to be put on such studies, and combinations of theoretical, modelling and animal applications could one day end with human implementations that would bring new and much more effective DBS techniques. The work presented in this study aims to show the importance of dedicating time and resources to such efforts and to highlight the importance of correlation and decorrelation in DBS.

5 References

[1] Global, regional, and national incidence, prevalence, and years lived with disability for 310 diseases and injuries, 1990–2015: a systematic analysis for the Global Burden of Disease Study 2015 (2016). Lancet; 388: 1545–602.

[2] William Dauer , Serge Przedborski (2003) Parkinson's Disease: Mechanisms and Models. Neuron, Vol. 39, 889–909.

[3] Constance Hammond, Hagai Bergman and Peter Brown (2007) Pathological synchronization in Parkinson's disease: networks, models and treatments. Trends Neurosci;30(7):357-64

[4] Christian Hauptmann and Peter A Tass (2010). Restoration of segregated, physiological neuronal connectivity by desynchronizing stimulation. J Neural Eng; 7(5):056008

[5] The deep-brain stimulation for parkinson's disease study group (2001). Deep-brain stimulation of the subthalamic nucleus or the pars interna of the globus pallidus in Parkinson's disease. N Engl J Med; 345(13):956-63

[6] P Limousin, P Pollak, A Benazzouz, D Hoffmann, J F Le Bas, E Broussolle, J E Perret and A L Benabid (1995) Effect of parkinsonian signs and symptoms of bilateral subthalamic nucleus stimulation. Lancet 4;345(8942):91-5

[7] Salvatore Galati, Paolo Mazzone, Ernesto Fedele, Antonio Pisani, Antonella Peppe, Mariangela Pierantozzi, Livia Brusa, Domenicantonio Tropepi, Vincenzo Moschella, Maurizio Raiteri, Paolo Stanzione, Giorgio Bernardi and Alessandro Stefani (2006) Biochemical and electrophysiological changes of substantia nigra pars reticulata driven by subthalamic stimulation in patients with Parkinson's disease. Eur J Neurosci;23(11):2923-8

[8] A. Benazzouz, D.M. Gao, Z.G. Ni, B. Piallat, R. Bouali-Benazzouz and L. Benabid (2000) Effect of high-frequency stimulation of the subthalamic nucleus on the neuronal activities of the substantia

nigra pars reticulata and ventrolateral nucleus of the thalamus in the rat. Neuroscience ;99(2):289-95

[9] Philip J. Hahn, Gary S. Russo, Taka Hashimoto, Svjetlana Miocinovic, Weidong Xu, Cameron C. McIntyre and Jerrold L. Vitek (2008) Pallidal burst activity during therapeutic deep brain stimulation. Experimental Neurology 211 243–251

[10] Mark D. Humphries and Kevin Gurney (2012) Network effects of subthalamic deep brain stimulation drive a unique mixture of responses in basal ganglia output. European Journal of Neuroscience, Vol. 36, pp. 2240–2251

[11] R L Albin, A B Young and J B Penney (1989) The functional anatomy of basal ganglia disorders. Trends Neurosci (10):366-75

[12] Leonid L. Rubchinsky, Nancy Kopell, and Karen A. Sigvardt (2003). Modeling facilitation and inhibition of competing motor programs in basal ganglia subthalamic nucleus–pallidal circuits. PNAS, 2003 100 (24) 14427-14432

[13] Deniau JM and Chevalier G (1985). Disinhibition as a basic process in the expression of striatal functions. II. The striato-nigral influence on thalamocortical cells of the ventromedial thalamic nucleus. Brain Research, 334(2):227-233

[14] Robert Schmidt, Daniel K Leventhal, Nicolas Mallet, Fujun Chen and Joshua D Berke (2013). Canceling actions involves a race between basal ganglia pathways. Nat Neurosci;16(8):1118-24

[15] Jeongjin Kim et al (2017) Inhibitory Basal Ganglia Inputs Induce Excitatory Motor Signals in the Thalamus. Neuron Volume 95, Issue 5, Pages 1181-119

[16] R Llinás and H Jahnsen (1982) Electrophysiology of mammalian thalamic neurones in vitro. Nature . 1982 Jun 3;297(5865):406-8

[17] Mohammadreza Mohagheghi Nejad, Stefan Rotter and Robert Schmidt (2018) Transmission of motor signals from the basal ganglia to the thalamus: effect of correlations, sensory responses, and

excitation. DOI: 10.1101/386920

[18] Alexandre Kuhn, Ad Aertsen and Stefan Rotter (2003) Higher-order statistics of input ensembles and the response of simple model neurons. Neural Comput; 15(1):67-101

[19] Jens Volkmann (2004) Deep brain stimulation for the treatment of Parkinson's disease. J Clin Neurophysiol ;21(1):6-17.

[20] P Limousin, J D Speelman, F Gielen and M Janssens (1999) Multicentre European study of thalamic stimulation in parkinsonian and essential tremor. J Neurol Neurosurg Psychiatry; 66(3):289-96

[21] John Gardner (2013) A history of deep brain stimulation: Technological innovation and the role of clinical assessment tools. Soc Stud Sci ; 43(5): 707–728

[22] Christian Hauptmann, Peter A Tass (2010) Restoration of segregated, physiological neuronal connectivity by desynchronizing stimulation. J Neural Eng; 7(5):056008

[23] H Bergman, A Feingold, A Nini, A Raz, H Slovin, M Abeles, E Vaadia (1998) Physiological aspects of information processing in the basal ganglia of normal and parkinsonian primates. Trends Neurosci ;21(1):32-8

[24] E.Shink, M.D.Bevan, J.P.Bolam, Y.Smith (1998) Physiological aspects of information processing in the basal ganglia of normal and parkinsonian primates. Neuroscience ;73(2):335-57

[25] Mathias Pessiglione, Dominique Guehl, Anne-Sophie Rolland, Chantal François, Etienne C Hirsch, Jean Féger, Léon Tremblay (2005) Thalamic neuronal activity in dopamine-depleted primates: evidence for a loss of functional segregation within basal ganglia circuits. J Neurosci ;25(6):1523-31

[26] P. A. Tass, A. N. Silchenko, C. Hauptmann, U. B. Barnikol, and E.-J. Speckmann (2009) Long-lasting desynchronization in rat hippocampal slice induced by coordinated reset stimulation. Phys. Rev. E 80, 011902

[27] Jing Wang, Shane Nebeck, Abirami Muralidharan, Matthew D. Johnson, Jerrold L. Vitek and Kenneth B. Baker (2016). Coordinated Reset Deep Brain Stimulation of Subthalamic Nucleus

Produces Long-Lasting, Dose-Dependent Motor Improvements in the 1-Methyl-4-phenyl-1,2,3,6-tetrahydropyridine Non-Human Primate Model of Parkinsonism. Brain Stimulation 9 609–617.

6 Appendices

6.1 Scatterplots for deep brain stimulation simulations with decorrelation

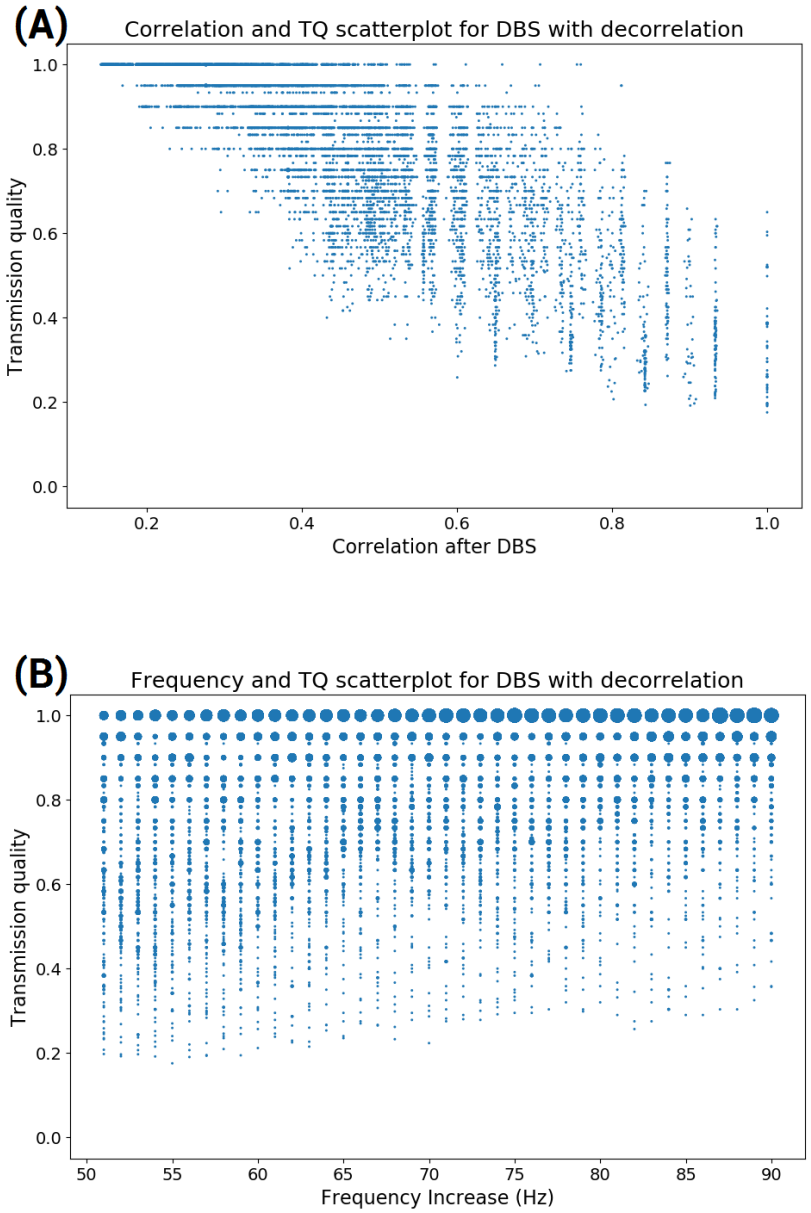

Figure 15. *Scatterplots for TQ, correlation and frequency increase for DBS with decorrelation* Circle size in both scatterplots denote the frequency of that specific combination of values. (A) plots TQ against correlation during DBS, where the correlation was for all 30 spiketrains. (B) Plots TQ against the firing rate of the group of decorrelated neurons

6.2 Scatterplots for deep brain stimulation simulations with no decorrelation

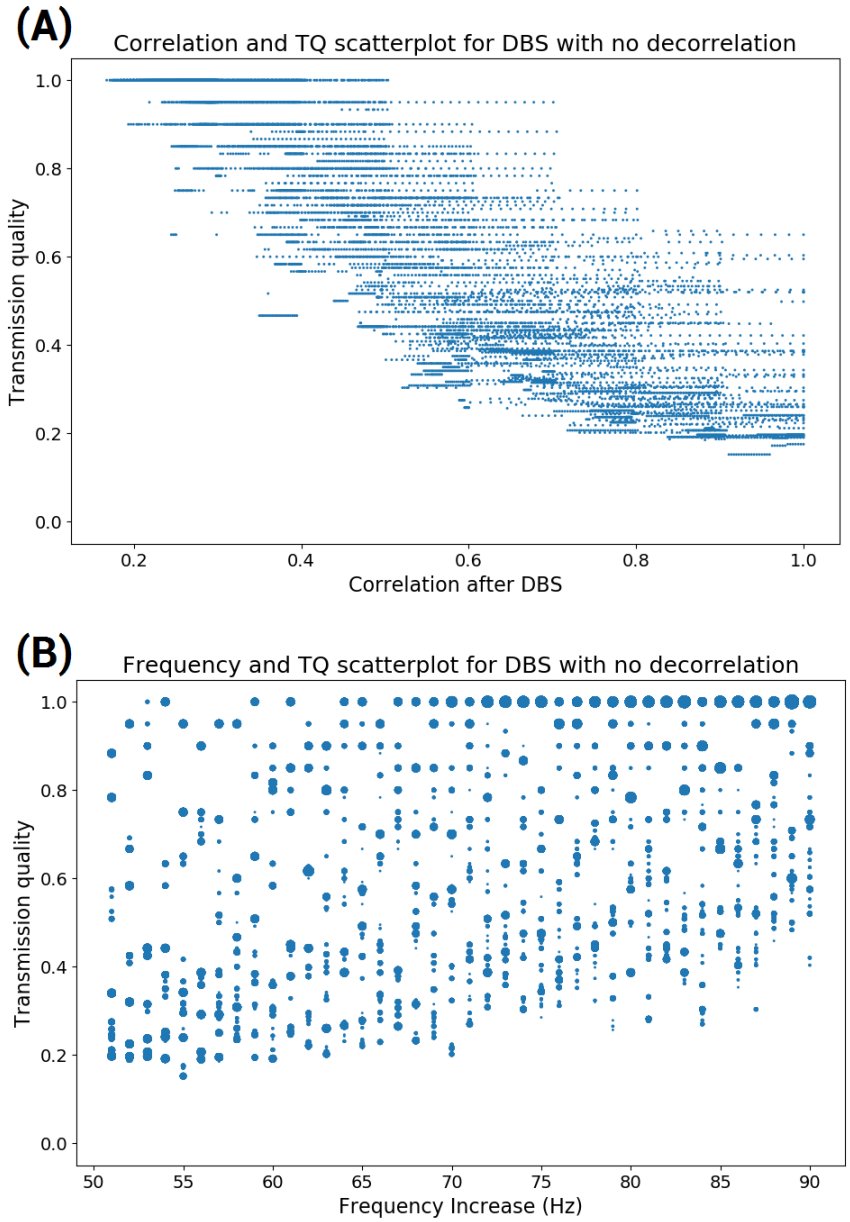

Figure 16. *Scatterplots for TQ, correlation and frequency increase for DBS with no decorrelation* Circle size in both scatterplots denote the frequency of that specific combination of values. (A) plots TQ against correlation during DBS, where the correlation was for all 30 spiketrains. (B) Plots TQ against the firing rate of the group of neurons affected by DBS

6.3 Scatterplots for deep brain stimulation simulations with 3 decorrelated neurons

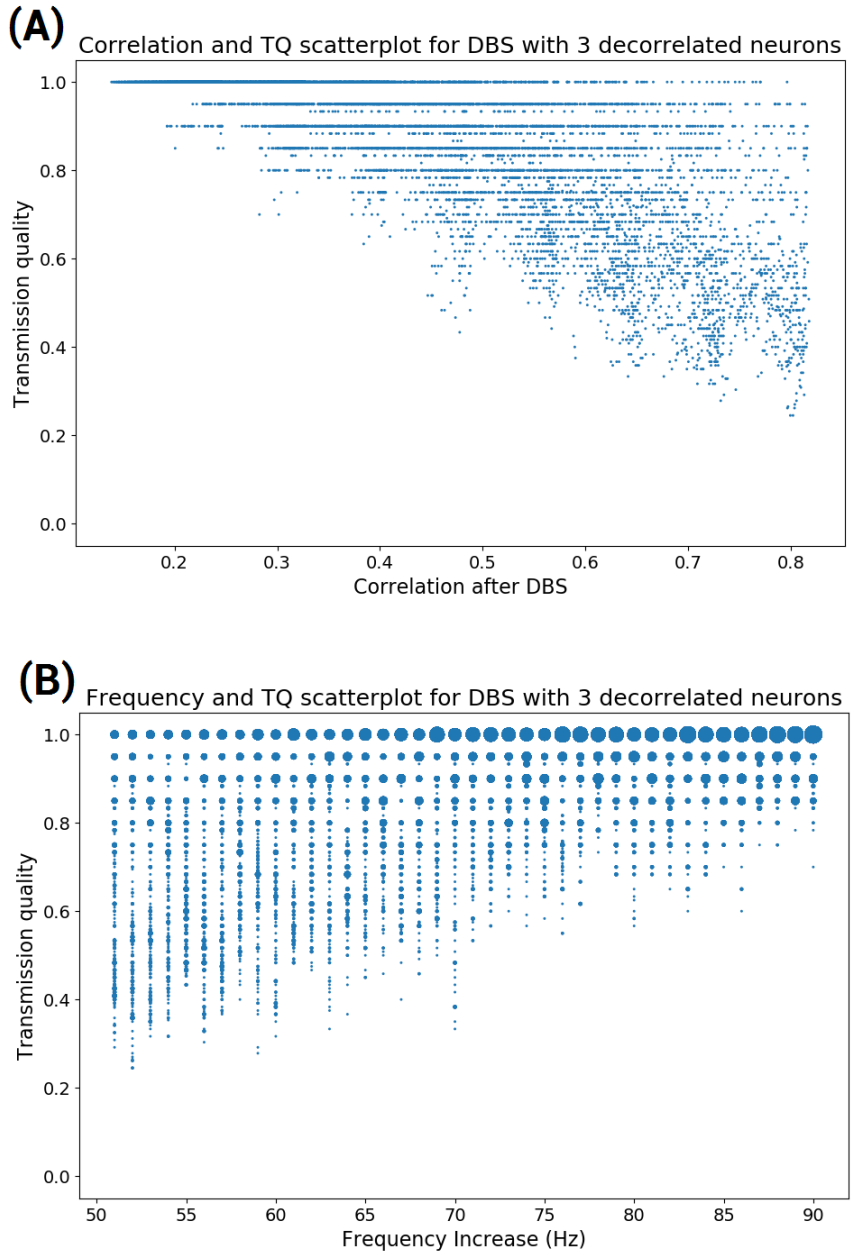

Figure 17. *Scatterplots for TQ, correlation and frequency increase for DBS with 3 decorrelated neurons* Circle size in both scatterplots denote the frequency of that specific combination of values. (A) plots TQ against correlation during DBS, where the correlation was for all 30 spiketrains). (B) Plots TQ against the firing rate of the group affected by DBS, including the 3 decorrelated neurons.